Journal of Power Sources 254 (2014) 190–197

Contents lists available at ScienceDirect

Journal of Power Sources

journal homepage: www.elsevier.com/locate/jpowsour

Unexpected high power performance of atomic layer deposition coated $Li[Ni_{1/3}Mn_{1/3}Co_{1/3}]O_2$ cathodes

Ji Woo Kim [a], Jonathan J. Travis [b], Enyuan Hu [c], Kyung-Wan Nam [c], Seul Cham Kim [d], Chan Soon Kang [d], Jae-Ha Woo [a], Xiao-Qing Yang [c], Steven M. George [a,b], Kyu Hwan Oh [d,*], Sung-Jin Cho [e,*], Se-Hee Lee [a,*]

[a] Department of Mechanical Engineering, University of Colorado at Boulder, Boulder, CO 80309-0427, USA
[b] Department of Chemistry & Biochemistry, University of Colorado at Boulder, Boulder, CO 80309-0215, USA
[c] Chemistry Department, Brookhaven National Laboratory, Upton, NY 11973, USA
[d] Department of Materials Science and Engineering, Seoul National University, Seoul 151-742, Republic of Korea
[e] Advanced Power Solution, Johnson Controls Inc., Milwaukee, WI 53209, USA

HIGHLIGHTS

- We applied Al_2O_3-ALD coating to a spotlighted cathode NMC material.
- The superior rate capability of the NMC/4ALD cell is well maintained.
- The preserved surface and crystal structures results in the improved kinetics.

ARTICLE INFO

Article history:
Received 13 November 2013
Received in revised form
26 December 2013
Accepted 27 December 2013
Available online 8 January 2014

Keywords:
Energy storage
Lithium nickel–manganese–cobalt oxide
Atomic layer deposition
Rate capability
High temperature cycle-life

ABSTRACT

Electric-powered transportation requires an efficient, low-cost, and safe energy storage system with high energy density and power capability. Despite its high specific capacity, the current commercially available cathode material for today's state-of-art Li-ion batteries, lithium nickel–manganese–cobalt oxide $Li[Ni_{1/3}Mn_{1/3}Co_{1/3}]O_2$ (NMC), suffers from poor cycle life for high temperature operation and marginal rate capability resulting from irreversible degradation of the cathode material upon cycling. Using an atomic-scale surface engineering, the performance of $Li[Ni_{1/3}Mn_{1/3}Co_{1/3}]O_2$ in terms of rate capability and high temperature cycle-life is significantly improved. The Al_2O_3 coating deposited by atomic layer deposition (ALD) dramatically reduces the degradation in cell conductivity and reaction kinetics. This durable ultra-thin Al_2O_3-ALD coating layer also improves stability for the NMC at an elevated temperature (55 °C). The experimental results suggest that a highly durable and safe cathode material enabled by atomic-scale surface modification could meet the demanding performance and safety requirements of next-generation electric vehicles.

1. Introduction

$LiNi_{1/3}Mn_{1/3}Co_{1/3}O_2$ (NMC) cathodes have been the subject of extensive studies as high-energy cathode materials for rechargeable Li-ion batteries because of their high specific capacity and relatively low cost [1–5]. However, practical use of NMC cathodes, particularly in plug-in hybrid electric vehicles (PHEVs) and electric vehicles (EVs), have been delayed because of their limited power performance (rate capability) and drastic degradation in their capacity and cycle-life at high operation temperatures (45 °C–60 °C) and voltages (>4.3 V) [6–8]. One possible way to endow NMC based cathodes with quality power performance is to blend them with a compensating cathode material, such as $LiMn_2O_4$ spinel (LMO), which has better high rate performance. This blending method enables use of NMC:LMO hybrid cathodes for less expensive commercialized electric vehicles (e.g. GM-Volt) [9] with improved power density and safety. However, emerging concerns about LMO's lower energy density compared to NMC and capacity fade due to metallic dissolution at elevated temperatures [10,11] has led to a need for researchers to develop new materials technology.

* Corresponding authors.
E-mail addresses: kyuhwan@snu.ac.kr (K.H. Oh), Sung-Jin.Cho@jci.com (S.-J. Cho), sehee.lee@colorado.edu (S.-H. Lee).

0378-7753/$ – see front matter © 2014 Elsevier B.V. All rights reserved.
http://dx.doi.org/10.1016/j.jpowsour.2013.12.119

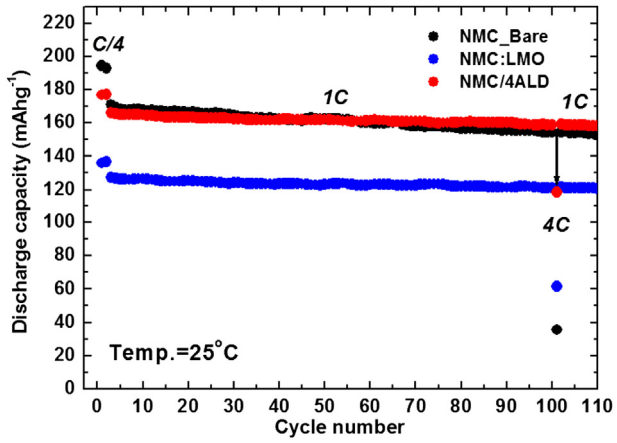

Fig. 1. Cycling performance of half cells using uncoated-NMC (NMC Bare), uncoated-NMC:LMO (NMC:LMO, 1:1 mixture) and Al_2O_3 4ALD coated-NMC (NMC/4ALD) cathodes cycled between 3.0 and 4.5 V versus Li^+/Li at 25 °C at 1 C-rate (160 mA g^{-1} for NMC Bare and NMC/ALD and 130 mAg^{-1} for NMC:LMO) following after the first two formation cycles at C/4-rate (40 mAg^{-1} for NMC Bare and NMC/ALD and 32.5 mAg^{-1} for NMC:LMO). Discharge capacities at 4C-rate (640 mAg^{-1} for NMC Bare and NMC/ALD and 520 mAg^{-1} for NMC:LMO) after 100 cycles are shown at the 101st cycle.

The demand for durable cathode materials has stimulated the use of many coating methods in order to protect the electrodes. One coating method, namely "sol–gel" wet-chemical process, has been employed to deposit various materials [12–16]. The high temperature cycle-life and safety issues of NMC and LMO based cathodes are greatly improved by means of the "sol–gel" coating process. However, a tradeoff between cycle-life and energy/power-density seems to be inevitable in the case of "sol–gel" coated cathodes. This is because the thickness of the protective coating layer on the cathode surface, which can be controlled but typically is a few nanometers thick, hinders the transport of electrons (e^-) and lithium ions (Li^+) across the coating layer during charge/discharge. This leads to the loss of initial capacity and poor performance at higher charge/discharge rates.

Recently, our group demonstrated atomic layer deposition (ALD) as an advanced coating method for a variety of Li-ion battery electrodes. [17–20] ALD utilizes sequential and self-limiting surface reactions that enable tailored conformal coatings with Å-level thickness control [21]. An additional advantage of ALD is that it may be employed for both powders and also directly on fully fabricated electrodes. Unfortunately fundamental mechanism for the performance improvement of Li-ion battery via ALD surface modification has not been elucidated yet. We present, for the first time, true fundamental mechanistic understanding of atomic-scale surface modification based on significant characterization including electrochemical impedance spectroscopy (EIS), galvanostatic intermittent titration technique (GITT), transmission electron microscopy (TEM), and Synchrotron x-ray diffraction (SR-XRD).

2. Experimental

2.1. Atomic layer deposition

Al_2O_3 ALD films were grown directly on NMC powders (Johnson Controls Inc.) using a rotary reactor. For the Al_2O_3 ALD, Trimethylaluminum (TMA 97%) and HPLC (high performance liquid chromatography) grade H_2O was purchased from Sigma–Aldrich. The typical growth rate for the chemistry is 1.1 Å per cycle. Due to a small amount of H_2O residue in the reactor after each cycle a slightly increased growth rate of 1.3 Å per cycle was achieved. The Al_2O_3 ALD reaction sequence was: i) TMA dose to 1.0 Torr; ii) hold pressure static for 60 s; iii) evacuation of reaction products and excess TMA; iv) 5 N_2 purges; v) H_2O dose to 1.0 Torr; vi) hold pressure static for 60 s; vii) evacuation of reaction products and excess H_2O; viii) and 5 N_2 purges. Each N_2 purge consisted of dosing N_2 to 20 Torr, holding pressure static for 60 s, and then pumping the

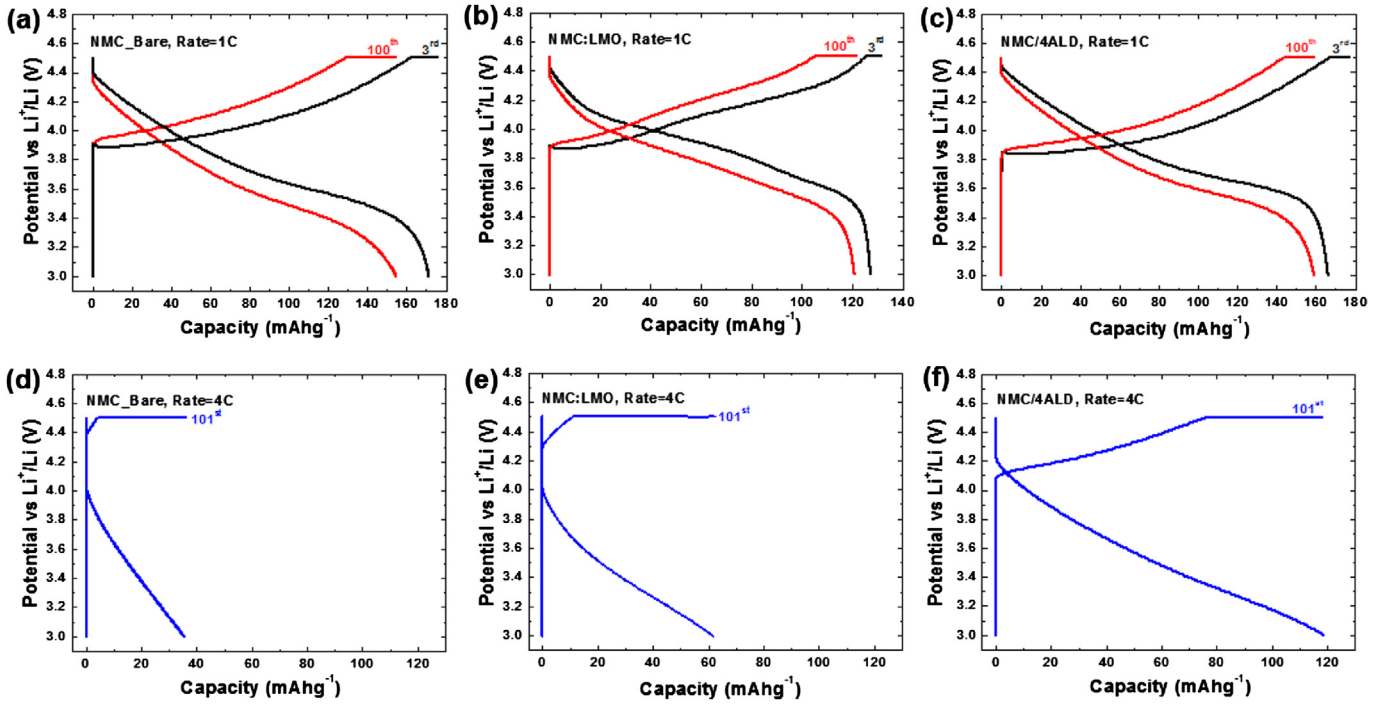

Fig. 2. (a–c) Comparison of 3rd and 100th charge–discharge voltage profiles (3.0–4.5 V) at 1 C-rate, (d–f) charge–discharge voltage profiles at 4 C-rate after continuous 100 cycles at 1 C-rate of NMC Bare, NMC:LMO and NMC/4ALD half cells. Voltage hold is applied at 4.5 V for 0.5 h after each charge step.

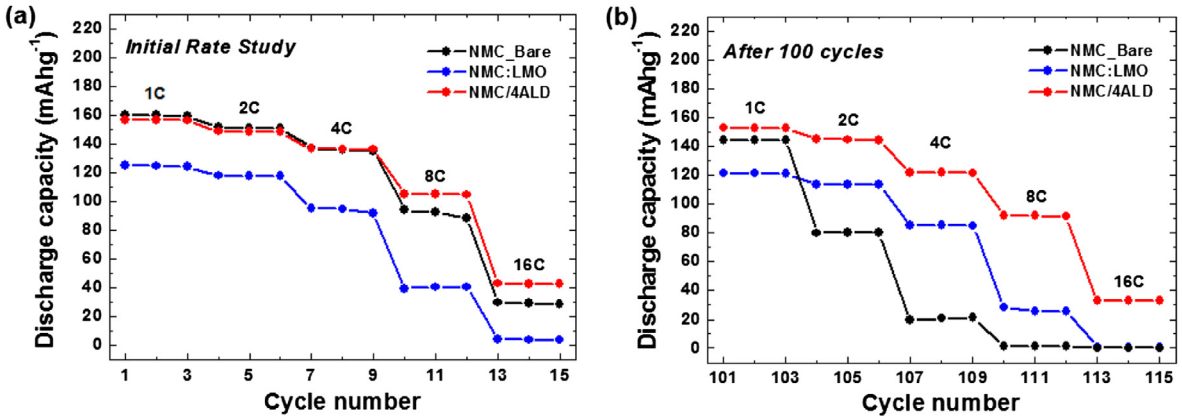

Fig. 3. Comparison of rate capabilities between NMC Bare, NMC:LMO and NMC/4ALD (a) initial rate tests and (b) rate tests after 100 cycles at 1 C-rate. The charge–discharge current density gradually increased by 160 mAg^{-1} (1 C), 320 mAg^{-1} (2 C), 640 mAg^{-1} (4 C), 1280 mAg^{-1} (8 C) and 2560 mAg^{-1} (16 C) for NMC Bare and NMC/4ALD; 130 mAg^{-1} (1 C), 260 mAg^{-1} (2 C), 520 mAg^{-1} (4 C), 1040 mAg^{-1} (8 C) and 2080 mAg^{-1} (16 C) for NMC:LMO with voltage hold at 4.5 V for 0.5 h after each charge step.

reaction chamber down for 60 s. This sequence constitutes one cycle of Al_2O_3 ALD. All ALD cycles were conducted at 180 °C. The Al_2O_3-coated NMC powders with 4 cycles of ALD (NMC/4ALD) were followed by heat treatment at 300 °C in Air for 12 h.

2.2. Electrochemical tests

Composite electrodes were comprised of the prepared powders (NMC Bare, NMC/4ALD and NMC:LMO = 1:1), carbon black and

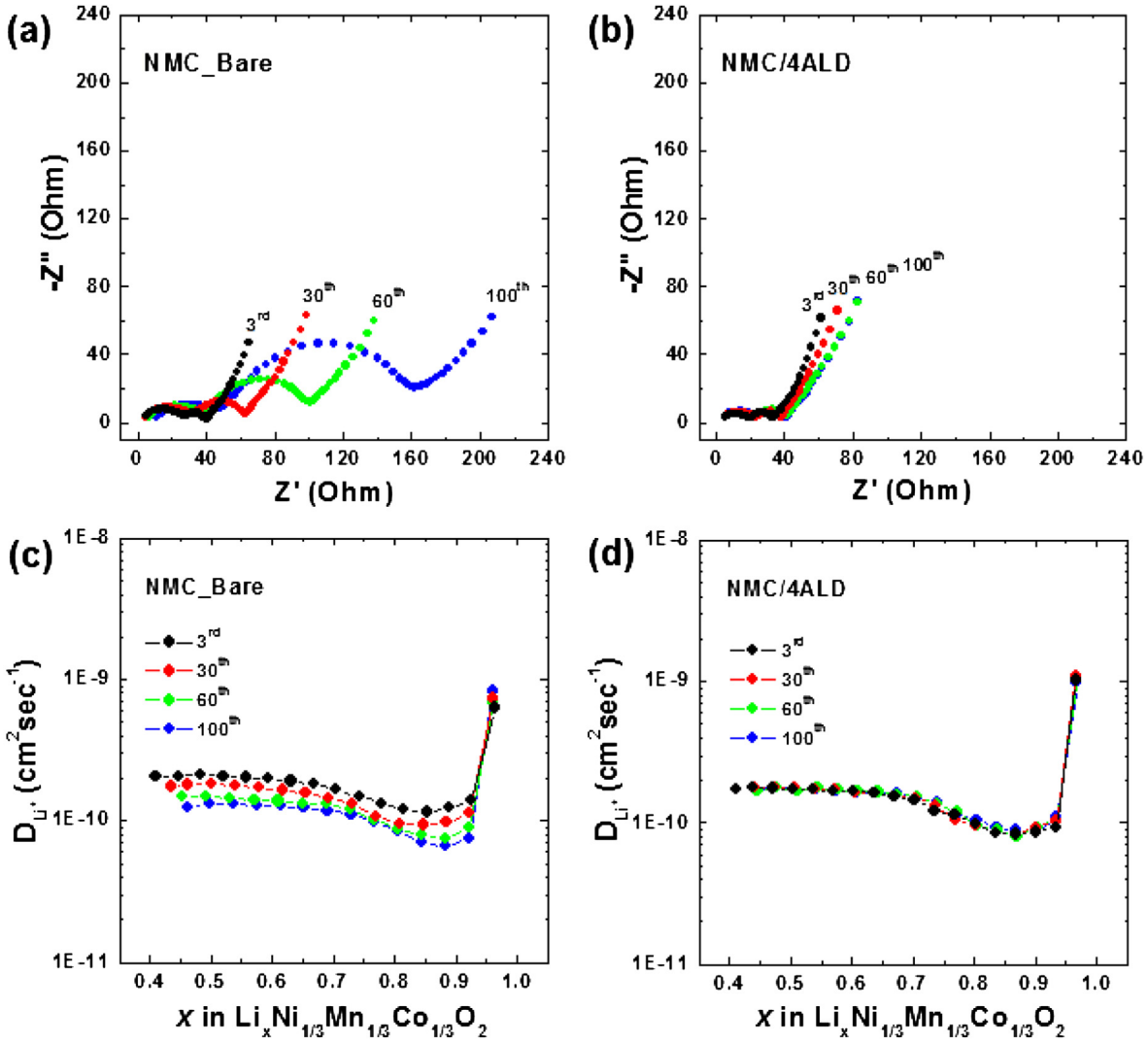

Fig. 4. Nyquist plots of fully charged (a) NMC Bare, (b) NMC/4ALD electrodes at 4.5 V, and variation of Li-ion diffusion coefficient (D_{Li}^{+}) measured by GITT as a function of Li content in (c) NMC Bare and (d) NMC/4ALD electrodes at 3rd, 30th, 60th and 100th cycle (1 C-rate, 3.0–4.5 V).

polyvinylidene fluoride (90:5:5) in *N*-methylpyrrolidinon. The composite was coated onto high grade Al foil current collector and roll-pressed after dried in air at 80 °C for 1 h. The electrodes were dried in a vacuum oven at 120 °C for 12 h before use. The separators were thick porous silica and the electrolyte was 1 M $LiPF_6$ in EC:DEC (1:1 volume ratio). Cell tests were done with a 2032 coin-type cell using Li metal as the anode.

All assembled cells were allowed to rest for at least 10 h at room temperature prior to electrochemical tests. For cycle-life tests, the cells were cycled between 3.0 and 4.5 V at low rate of C/4 (40 mAg^{-1}) during the initial two cycles. The cells were charged and discharged between 3.0 and 4.5 V by applying a constant 1 C current (160 mA^{-1}) and 30 min voltage hold at 4.5 V. The cycle-life tests at 55 °C were performed at both 3.0–4.3 V and 3.0–4.5 V with the same constant current (1 C-rate, 160 mAg^{-1}). Rate studies were tested (3.0–4.5 V) using a symmetric galvanostatic profile with the current systematically increased (160–320–640–1280–2560 mAg^{-1} for NMC Bare and NMC/4ALD cells and 130–260–520–1040–2080 mAg^{-1} for NMC:LMO) every three cycles and 30 min voltage hold at 4.5 V. AC impedance was performed using a Solatron 1280C for a frequency range of 20,000–0.0025 Hz. Impedance measurements were taken on 3rd, 30th, 60th and 100th cycle (1 C-rate cycling, 3.0–4.5 V) at fully charged state. For galvanostatic intermittent titration technique (GITT) measurements, a constant current flux was supplied for 2250 s (~C/10-rate) followed by an open circuit stand of the cell for 3600 s. This procedure was continued for the full charge voltage range (3.0–4.5 V) varying composition *x* in $Li_x(Ni_{1/3}Co_{1/3}Mn_{1/3})O_2$ and repeated at 3rd, 30th, 60th and 100th cycle during 1 C-rate cycling.

2.3. Microstructure characterizations

Cross-sectional samples were prepared from the 100 cycled (1 C-rate, 3.0–4.5 V) fully charged NMC Bare and NMC/4ALD electrodes using a dual-beam focused ion beam (FEI, Nova Nanolab 200). In order to analyze crystal structure of the both electrodes, TEM samples were prepared from the cross-sectioned electrode particles using a focused ion beam lift-out technique with a manipulating probe (Omniprobe 100.7). Crystal structure information from the inner area and outer area of each electrode TEM sample was determined by selected area electron diffraction (SAED) patterns using a high-resolution TEM (JEOL, JEM 3000F).

2.4. X-ray diffraction analysis

XRD data was collected at beamline X14A ($\lambda = 0.7788$ Å) at the National Synchrotron Light Source at Brookhaven National Laboratory (NSLS-BNL). The data were collected with glass capillaries (0.5 mm diameter) in transmission mode using a silicon strip detector scanning from 6 to 60° two-theta. To prepare ex-situ samples, cells are disassembled in Argon-filled glove box and electrodes are washed and scratched off the current collector. They are sealed in glass capillaries in the glove box to avoid air exposure. For easy comparison with other researchers' results, all two theta values in the XRD data are converted to the two-theta value of Cu Kα wavelength ($\lambda = 1.5418$ Å). Rietveld refinements were performed on the collected data using GSAS-EXPGUI software.

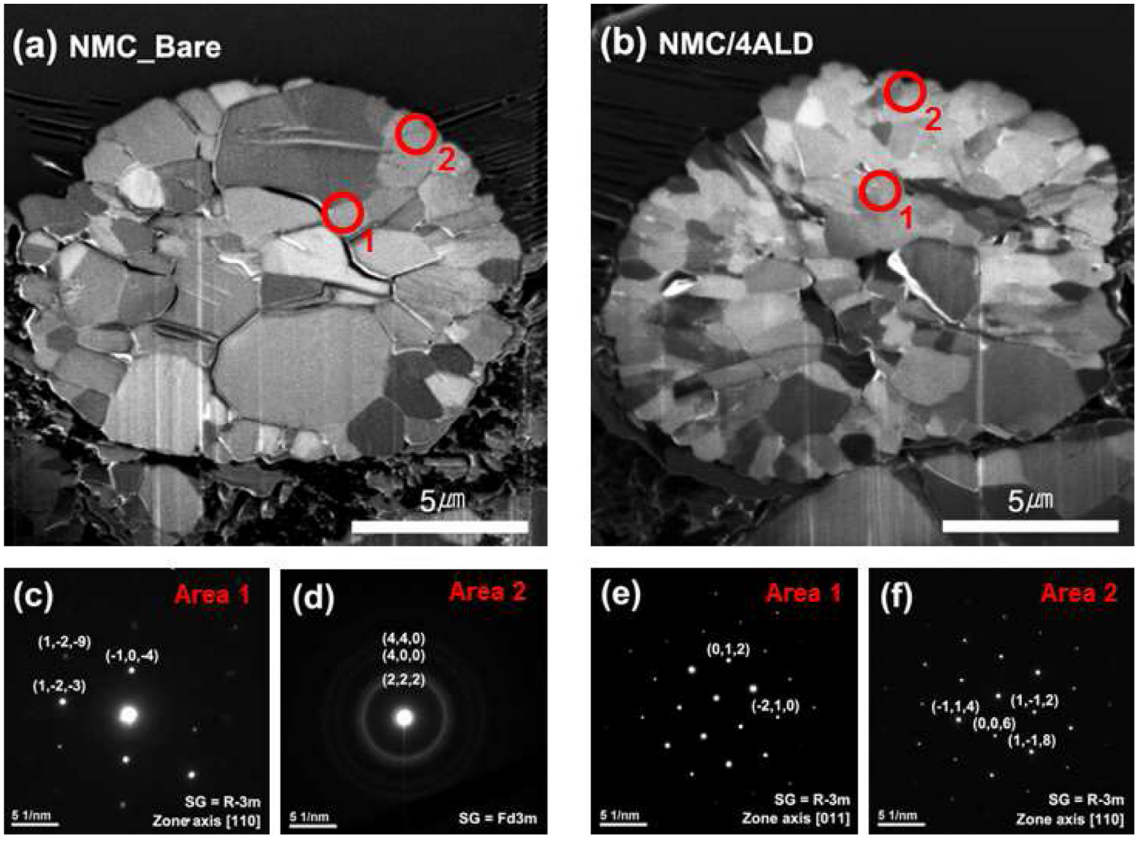

Fig. 5. FIB cross-section images of fully charged (delithiated) (a) NMC Bare and (b) NMC/4ALD after 100 cycles at 1 C-rate between 3.0 and 4.5 V. TEM selected area electron diffraction (SAED) patterns from inner area (1) and outer area (2) of each particle show phase transition in NMC Bare electrode (c,d) whereas NMC/4ALD presents same crystal structure from inner and outer area (e,f).

3. Results and discussion

Uncoated NMC (NMC Bare), 1:1 mixture of NMC:LMO (NMC:LMO), and NMC/4ALD electrodes were tested in CR2032 coin cells with Li-metal foil anode. Fig. 1 shows a cycling performance of the three battery cells at room temperature (25 °C) between 3.0 and 4.5 V at 1 C-rate after the two formation cycles at C/4-rate. When charged/discharged at 1 C-rate (160 mAg^{-1}) at the initial stage, the NMC Bare cell delivers a discharge capacity of approximately 171 mAh/g while the NMC/4ALD cell shows a slightly lower capacity of 166 $mAhg^{-1}$. The initial lower capacity of the NMC/4ALD was expected due to the additional Al_2O_3 coating layer on the surface of the cathode particles. The Al_2O_3 layer may affect ionic mobility through the coating layer although the thickness of the layer is ultra-thin (<1 nm). During the 1 C-rate cycling from 3rd to 100th cycle, the NMC/4ALD cell exhibits cycling performance with the highest capacity retention, 96% of the initial capacity, which surpasses the NMC Bare (91%) and the NMC:LMO (95%) cells. It is notable that the discharge capacity of the NMC/4ALD starts to overtake the NMC Bare at around the 50th cycle. The NMC:LMO electrode cell, which is currently being used for Li-ion batteries in commercial PHEVs, exhibits a moderate initial capacity (127 $mAhg^{-1}$) and cyclability (95%) as expected. The NMC/4ALD, however, still appears to be more attractive in terms of the Li-ion batteries' specific energy density. The charge/discharge voltage profiles of the NMC Bare, NMC:LMO and NMC/4ALD cells at 3rd and 100th cycle with 1 C-rate are shown in Fig. 2a–c displaying stable voltage potentials and capacities corresponding to the passable capacity retentions after the continuous 1 C-rate cycling.

Surprisingly, the most striking result is observed at 4 C-rate cycling at the 101st cycle right after the consecutive 100 cycles with 1 C-rate as seen in Fig. 1. Although the pristine NMC Bare and the NMC/4ALD cells have shown a similar discharge capacity (~160 $mAhg^{-1}$) at 1 C-rate cycling, there is a huge difference in the specific capacity ($\Delta Cap.$ = 83 $mAhg^{-1}$) between the two cells recorded at four times higher current density (4 C-rate, 640 mAg^{-1}). In Fig. 2d and f, the voltage profiles of NMC/4ALD show a significantly reduced overpotential compared to the NMC Bare between the 1 C-rate and the 4 C-rate cycling. This leads to a higher capacity of 118 mAh g^{-1} for NMC/4ALD in contrast to a diminished capacity of 35 mAh g^{-1} for NMC Bare. The NMC/4ALD cell exhibits an excellent high-rate capability despite its high active material content (90% of the composite electrode). The NMC:LMO cell (Fig. 2e) also shows a reasonable rate capability with a discharge capacity of $mAhg^{-1}$, mainly due to the superior rate capability of the LMO, but this is still much less than that of the NMC/4ALD. The outstanding cycle-life and high-rate performance of the NMC/4ALD implies that the ALD Al_2O_3 coating enhances the electrochemical properties of the pristine NMC through nano-scale surface modification, the positive effects of which are maintained over the long-term cycling even at high current rate.

One of the reasons for the Li-ion battery manufacturers to hesitate to apply NMC solely as a cathode material to their high energy and power Li-ion battery is due to its inferior rate capability compared to LMO. Here we report the outstanding performances in charge/discharge rate capability of the NMC by the Al_2O_3 ALD coating, which could potentially enable the use of NMC in Li-ion batteries for next generation electric vehicles. Fig. 3 shows a

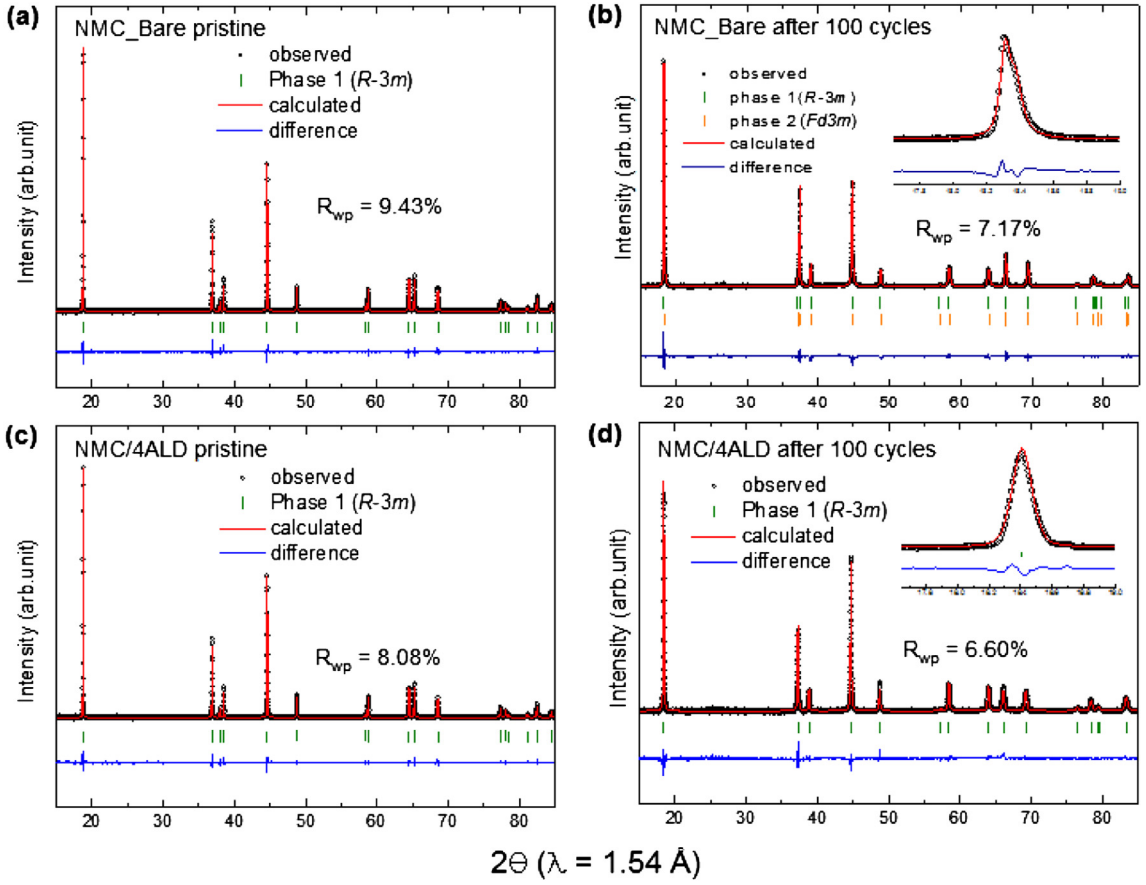

Fig. 6. Synchrotron X-ray diffraction patterns of fully charged (a,b) NMC Bare and (c,d) NMC/4ALD at 3rd cycle and 100th cycle respectively during 1 C-rate cycling test between 3.0 and 4.5 V.

comparison of rate capabilities of the three cells at the initial stage (a), and after the consecutive 100 cycles with 1 C-rate (b) in a voltage range of 3.0–4.5 V. For each different rate step, a constant current density was equally applied for both charge and discharge (160 mAg^{-1} (1 C), 320 mAg^{-1} (2 C), 640 mAg^{-1} (4 C), 1280 mAg^{-1} (8 C) and 2560 mAg^{-1} (16 C) for NMC Bare and NMC/4ALD cells, 130 mAg^{-1} (1 C), 260 mAg^{-1} (2 C), 520 mAg^{-1} (4 C), 1040 mAg^{-1} (8 C) and 2080 mAg^{-1} (16 C) for NMC:LMO). Note that a voltage was held at 4.5 V for 30 min after each charge process. At the initial stage of the rate tests in Fig. 3a the NMC Bare and the NMC/4ALD show a similar rate capability up to 4 C-rate. However, when the cells are discharged with 8 C-rate and 16 C-rate, the NMC Bare shows lower discharge capacities of 92 $mAhg^{-1}$ and 30 $mAhg^{-1}$ respectively whereas the NMC/4ALD cell delivers higher discharge capacities of 105 $mAhg^{-1}$ and 43 $mAhg^{-1}$. It is highly remarkable that the NMC/4ALD cell still can deliver higher capacity at 4 C-rate (~137 $mAhg^{-1}$) than the commercialized NMC:LMO cell at 1 C-rate (~125 $mAhg^{-1}$) which means the NMC/4ALD can be charged/discharged four times faster than the commercialized NMC:LMO cathode battery even together with a higher energy density. To check the stability of the rate capability, the same test protocols were applied to the three cells after 100 consecutive cycles at 1 C-rate. As seen in Fig. 3b, the superior rate capability of the NMC/4ALD cell is well maintained (121 $mAhg^{-1}$ at 4 C-rate) whereas the NMC Bare drastically degrades at the same rate (20 $mAhg^{-1}$ at 4 C-rate). The NMC:LMO cell is still delivering a tolerable capacity of 85 $mAhg^{-1}$ at 4 C-rate, however it is obvious that the NMC/4ALD is a much more attractive cathode material to meet the energy and power requirements for electric vehicles.

The superior cycle-life and rate capability provided by the Al_2O_3-ALD coating are related to the modified surface characteristics such as interfacial charge-transfer process, and Li-ion diffusion kinetics in the bulk cathode material which can be inferred from Li-ion diffusion coefficient. In order to assess surface characteristics of the NMC Bare and the NMC/4ALD, EIS measurements were performed after the Li-ion extraction up to 4.5 V at the 3rd, 30th, 60th and 100th cycles during 1 C-rate cycling. Fig. 4a and b shows Nyquist plots for the NMC Bare and the Al_2O_3-coated NMC with increasing frequency from right (0.0025 Hz) to left (20,000 Hz). Each of the impedance spectra is composed of two semicircles in high to medium frequency range and a straight line at low frequencies. The semicircle at high frequency represents resistance of the solid electrolyte interface (R_{sf}) that covers cathode particles. The semicircle at medium frequency is associated with the charge-transfer resistance (R_{ct}). The most prominent differences between NMC Bare and NMC/4ALD are observed in the resistance of the surface films at the electrode/electrolyte interface (R_{sf}) and the charge-transfer resistance (R_{ct}). Compared to the small and steady R_{sf} and R_{ct} for NMC/4ALD electrode, the resistances of NMC Bare drastically increase with the consecutive 1 C-rate cycling.

GITT [22] was employed to evaluate the Li-ion diffusion kinetics in the bulk cathode particle. The Li-ion diffusion coefficients (D_{Li}^{+}) of each NMC Bare and NMC/4ALD at the 3rd, 30th, 60th and 100th cycles were recorded during charge process as seen in Fig. 4c and d. Continuous decrease in the Li-ion diffusion coefficient of the NMC Bare cell is clearly observed as a function of cycle number in contrast to the NMC/4ALD cell maintains its original Li-ion diffusion coefficient. These increased resistances and a slowdown in Li-ion

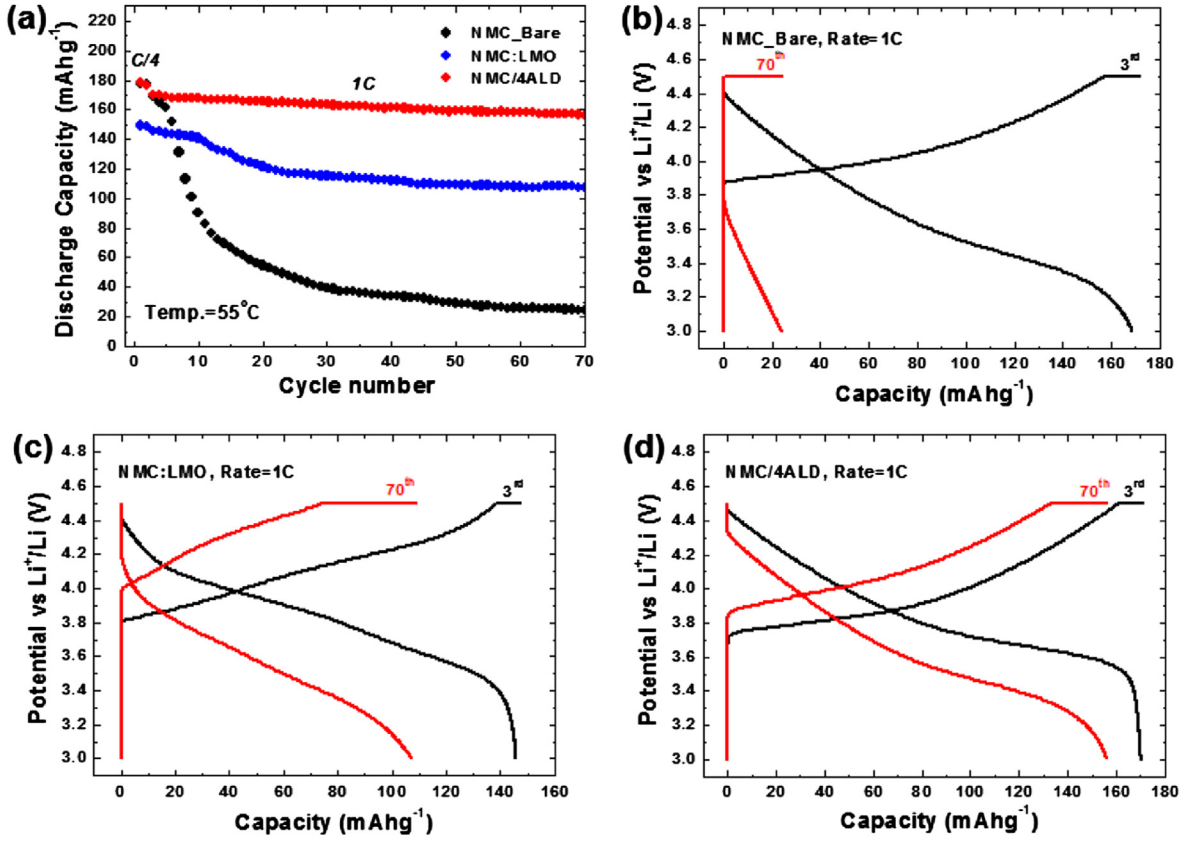

Fig. 7. (a) Cycling performance of half cells using uncoated-NMC (NMC Bare), uncoated-NMC:LMO (NMC:LMO, 1:1 mixture) and Al_2O_3 4ALD coated-NMC (NMC/4ALD) cathodes cycled between 3.0 and 4.5 V versus Li^+/Li at 55 °C by applying a constant rate of 1 C-rate (160 mAg^{-1} for NMC Bare and NMC/ALD and 130 mAg^{-1} for NMC:LMO) following after the first two formation cycles at C/4-rate (40 mAg^{-1} for NMC Bare and NMC/ALD and 32.5 mAg^{-1} for NMC:LMO). Comparison of 3rd and 70th charge–discharge voltage profiles (3.0–4.5 V) at 1 C-rate of (b) NMC Bare, (c) NMC:LMO and (d) NMC/4ALD half cells. Voltage hold was applied at 4.5 V for 0.5 h after each charge step.

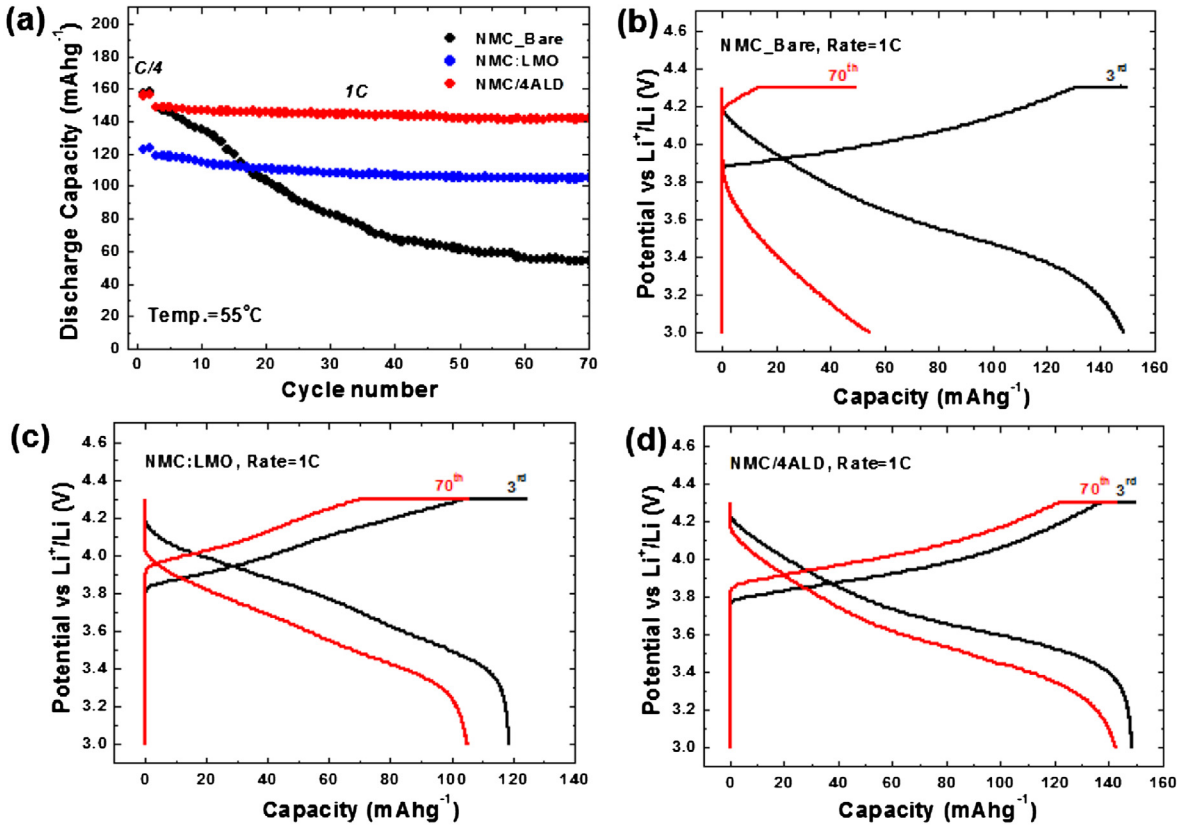

Fig. 8. (a) Cycling performance of half cells using uncoated-NMC (NMC Bare), uncoated-NMC:LMO (NMC:LMO, 1:1 mixture) and Al_2O_3 4ALD coated-NMC (NMC/4ALD) cathodes cycled between 3.0 and 4.3 V versus Li^+/Li at 55 °C by applying a constant rate of 1 C-rate (160 mAg^{-1} for NMC Bare and NMC/ALD and 130 mAg^{-1} for NMC:LMO) following after the first two formation cycles at C/4-rate (40 mAg^{-1} for NMC Bare and NMC/ALD and 32.5 mAg^{-1} for NMC:LMO). Comparison of 3rd and 70th charge–discharge voltage profiles (3.0–4.3 V) at 1 C-rate of (b) NMC Bare, (c) NMC:LMO and (d) NMC/4ALD half cells. Voltage hold was applied at 4.3 V for 0.5 h after each charge step.

kinetics are directly attributed to the decline in the cycle-life and rate performance of the NMC Bare electrode as observed in Figs. 1 and 2. Therefore, it is obvious that the bare NMC electrode undergoes degradation of its surface characteristics and Li-ion kinetics which eventually lead to deterioration of cell performance.

To check the effects of Al_2O_3 ALD coating on preservation of crystal structure of the NMC, a NMC Bare and NMC/4ALD particle was carefully selected from the 100 cycled (after delithiated to 4.5 V) electrode and analyzed by focused ion beam (FIB) and TEM. Fig. 5a and b shows FIB ion beam images of the cross-sectioned NMC Bare and NMC/4ALD particle. Average particle size of both the NMC Bare and NMC/4ALD is about 12 μm and each primary particle is composed of multiple grains with the size range of 1–5 μm. In Fig. 5c and d, TEM selected area electron diffraction (SAED) patterns show that NMC Bare electrode undergoes phase transition during 100 cycles from layered structure mother phase (space group: R-3m) to spinel cubic structure (space group: Fd3m). In contrast, the Al_2O_3-ALD coating layer preserves the original layered structure of NMC/4ALD electrode for the same cycling period as seen in Fig. 5e and f. In Fig. 6, SR-XRD and Reitveld refinement on the NMC/4ALD sample also confirm that there is no structural change in the NMC/4ALD electrode materials after 100 charge/discharge cycles at 1-C rate. In contrast, the diffraction peaks of NMC Bare electrode after 100 cycles feature great asymmetry. This result suggests that there could be composition inhomogeneity in the NMC bare sample after 100 cycles, leading to the formation of multiple phases. These phases could be developed at the surface of the particle during the cycling, accompanied by the breaking down of particles, yielding nano-sized particles that produce the ring pattern as seen in TEM analyses. Therefore we conclude that the excellent rate capability of the NMC/4ALD cell is mainly attributed to both preserved surface characteristics and crystal structures which are favorable to electrons and Li-ions transport during charge/discharge processes.

For a cathode material to meet the safety and energy requirements for Li-ion batteries in electric vehicles, the high temperature cycling performance of the cathode material must be ensured. To investigate high temperature performances of the three cells, NMC Bare, NMC:LMO and NMC/4ALD half cells are cycled at 55 °C with 1 C-rate between 3.0 and 4.5 V as seen in Fig. 7. The uncoated NMC (NMC Bare) exhibits a significant decline in the discharge capacity after a couple of initial cycles. The capacity retention from 3rd to 70th cycle is only 14% at 1 C-rate cycling (169 $mAhg^{-1}$ → 24 $mAhg^{-1}$), whereas the NMC/4ALD cell shows the best result with the highest retained capacity (92% of retention; 170 $mAhg^{-1}$ → 156 $mAhg^{-1}$) during the same cycling period. At lower voltage cut-off (3.0–4.3 V, 55 °C and 1 C-rate), the NMC/4ALD cell shows again an excellent cycling performance with 96% of capacity retention (148 $mAhg^{-1}$ → 142 $mAhg^{-1}$) in contrast to each NMC:LMO and NMC Bare cell only delivers 88% (119 $mAhg^{-1}$ → 105 $mAhg^{-1}$) and 36% (149 $mAhg^{-1}$ → 54 $mAhg^{-1}$) of its initial capacity as seen in Fig. 8.

4. Conclusion

We applied Al_2O_3-ALD coating to a spotlighted cathode material (NMC), which traditionally suffers from unacceptable rate capability and high temperature cycling performance thus necessitating

the battery manufactures to blend NMC with other compensating materials, despite its high capacity. With our coating method, the coated NMC cell delivered a high capacity (166 $mAhg^{-1}$, 3.0–4.5 V, 1 C-rate) and maintained excellent capacity retention over 96% during long-term cycling. At the same time, a demand for high power density was also satisfied by our ALD coating process with the improved rate capability of the coated NMC. This outstanding rate capability of the NMC/4ALD cell ($\sim$137 $mAhg^{-1}$ at 4 C-rate), which is four times faster than the NMC:LMO cell ($\sim$125 $mAhg^{-1}$ at 1 C-rate), demonstrates that the Al_2O_3-ALD coating layer dramatically prevents an increase in cell resistances and a slowdown in Li-ion kinetics by preserving the crystal structure of the NMC. This durable ultra-thin Al_2O_3-ALD coating layer also worked to improve stability for the NMC at an elevated temperature (55 °C). Thus we successfully obtained a remarkable capacity (170 $mAhg^{-1}$, 3.0–4.5 V, 1 C-rate) together with a high retention (92%) which is stable at high temperatures. We believe our work offers significant advantages to most of the layered lithium transition-metal oxide cathodes by addressing the raised issues; poor cycle-life, slow rate capability, and safety concerns at high temperature, without severe loss in their original energy density. Therefore, we anticipate that our work will spark much interest in Li-ion battery and electric vehicle manufacturers who are actively seeking high energy, power and safe cathode materials for Li-ion batteries.

Acknowledgments

This work was supported by the National Science Foundation (NSF, DMR-1206462). Work at Seoul National University was supported by a grant from the Fundamental R&D Program for Technology of World Premier Materials funded by the Ministry of Knowledge Economy, Republic of Korea (10037919). Work at Brookhaven National Lab. was supported by the U.S. Department of Energy, the Assistant Secretary for Energy Efficiency and Renewable Energy, Office of Vehicle Technologies under Contract No. DEAC02-98CH10886. The authors acknowledge technical supports by the beamline scientist Jianming Bai at beamline X14A of National Synchrotron Light Source, which is supported by the U.S. Department of Energy, Office of Science, Office of Basic Energy Sciences.

References

[1] N. Yabuuchi, T. Ohzuku, J. Power Sources 119–121 (2003) 171.
[2] I. Belharouak, Y.-K. Sun, J. Liu, K. Amine, J. Power Sources 123 (2003) 247.
[3] S. Jouanneau, K.W. Eberman, L.J. Krause, J.R. Dahn, J. Electrochem. Soc. 150 (2003) A1637.
[4] K.M. Shaju, P.G. Brucce, Adv. Mater. 18 (2006) 2330.
[5] I. Belharouak, W. Lu, D. Vissers, K. Amine, Electrochem. Commun. 8 (2006) 329.
[6] N. Yabuuchi, T. Ohzuku, J. Power Sources 146 (2005) 636.
[7] Z.H. Chen, Y.-K. Sun, K. Amine, J. Electrochem. Soc. 153 (2006) A1818.
[8] K. Amine, Z. Chen, Z. Zhang, J. Liu, W. Lu, Y. Qin, J. Lu, L. Curtis, Y.-K. Sun, J. Mater. Chem. 21 (2011) 17754.
[9] M. Alamgir, K. Yoo, B. Koetting, M. Klein, in: Presented at 2011 DOE Hydrogen Program and Vehicle Technologies Office Annual Merit Review and Peer Evaluation Meeting, Arlington, VA, 10 May 2011.
[10] M.M. Thackeray, Prog. Solids Chem. 25 (1997) 1.
[11] A. Blyr, C. Sigala, G. Amatucci, D. Guyornard, Y. Chabre, J.-M. Tarascon, J. Electrochem. Soc. 145 (1998) 194.
[12] S.-T. Myung, K. Izumi, S. Komaba, Y.-K. Sun, H. Yashiro, N. Kumagai, Chem. Mater. 17 (2005) 3695.
[13] S.B. Jang, S.-H. Kang, K. Amine, Y.C. Bae, Y.-K. Sun, Electrochim. Acta 50 (2005) 4168.
[14] Y. Kim, H.S. Kim, S.W. Martin, Electrochim. Acta 52 (2006) 1316.
[15] Y.-K. Sun, S.-W. Cho, S.-W. Lee, C.S. Yoon, K. Amine, J. Electrochem. Soc. 154 (2007) A168.
[16] S.-T. Myung, K. Amine, Y.-K. Sun, J. Mater. Chem. 20 (2010) 7074.
[17] Y.S. Jung, A.S. Cavanagh, A.C. Dillon, M.D. Groner, S.M. George, S.H. Lee, J. Electrochem. Soc. 157 (2010) A75.
[18] Y.S. Jung, A.S. Cavanagh, A.C. Dillon, M.D. Groner, S.M. George, S.H. Lee, Adv. Mater. 22 (2010) 2172.
[19] I.D. Scott, Y.S. Jung, A.S. Cavanagh, Y. Yan, A.C. Dillon, S.M. George, S.H. Lee, Nano Lett. 11 (2011) 414.
[20] L.A. Riley, S.V. Atta, A.S. Cavanagh, Y. Yan, S.M. George, P. Liu, A.C. Dillon, S.H. Lee, J. Power Sources 196 (2011) 3317.
[21] S.M. George, Chem. Rev. 110 (2010) 111.
[22] K.M. Shaju, G.V. Subba Rao, B.V.R. Chowdari, J. Electrochem. Soc. 151 (2004) A1324.